

Distortions from Octahedral Symmetry in Hypoelectronic Six-Vertex Polyhedral Clusters of the Group 13 Elements Boron, Indium, and Thallium as Studied by Density Functional Theory

R. B. King*

Department of Chemistry, University of Georgia,
Athens, Georgia 30602

I. Silaghi-Dumitrescu* and A. Kun

Faculty of Chemistry and Chemical Engineering,
Babeş-Bolyai University, Cluj-Napoca, Roumania

Received August 31, 2000

1. Introduction

Experimental work in recent years by Corbett and co-workers¹ on intermetallics containing alkali metals and the heavier group 13 elements indium and thallium (icosogens² or triels¹) has led to the discovery of a number of unusual deltahedra quite different from the deltahedra found in the boranes $B_nH_n^{2-}$ ($6 \leq n \leq 12$).^{3,4} This appears to be related to the skeletal electron counts of the cluster deltahedra,^{5–7} since borane deltahedra contain $2n + 2$ skeletal electrons whereas the icosogen deltahedra in the alkali metal intermetallics contain fewer than $2n + 2$ skeletal electrons and thus may be regarded as hypoelectronic. Such hypoelectronic deltahedra are known for icosogen clusters containing 6,^{8,9} 7,¹⁰ 9,¹¹ 10,^{12–14} and 11,^{15–19} atoms. An analysis of the topology of these hypoelectronic polyhedra^{20,21} suggests that the apparent electron deficiency is relieved by a distortion consisting of flattening selected degree 4 vertices of the parent deltahedron.

The work discussed in this paper represents an initial attempt to study computationally by modern density functional theory (DFT) methods the phenomenon of flattening in hypoelectronic icosogen deltahedra. Previous computational work on these deltahedra, largely by Corbett and co-workers,¹ has been limited to extended Hückel methods. The six-vertex system was selected

Table 1. Total Energies (au) of the Optimum Structures of Ic_6^{z-} Species

<i>z</i>	method	B_6^{z-}	In_6^{z-}	Tl_6^{z-}
4	B3LYP/LANL2DZ	−147.8860165	−10.8247947	−309.2358056
4	LSDA/pBP86/DN*	−148.00215	−34458.81919	
6	B3LYP/LANL2DZ	−146.5265194	−9.8979723	−308.2994419 ^d −308.2891499 ^e
6	LSDA/pBP86/DN*	−147.09378 ^a −146.62782 ^b −146.61358 ^c	−34457.90383	
8	B3LYP/LANL2DZ	−144.618819	−8.484888	−306.9061411 ^f
8	LSDA/pBP86/DN*	−144.65176	−34456.56989	

^a Linear ($D_{\infty h}$). ^b Bicapped tetrahedron (C_{2v}). ^c Oblate tetragonal bipyramid (D_{4h}). ^d Oblate trigonal antiprism (D_{3d}). ^e Single point calculation of a D_{4h} oblate tetragonal antiprism obtained from the octahedron by applying the same ratio of compression as achieved by optimized In_6^{6-} relative to In_6^{8-} . ^f Single point value calculated at the experimental geometry (O_h).

for this DFT study since it represents by far the least complicated of the icosogen deltahedra exhibiting flattening. The experimentally known examples of hypoelectronic six-vertex deltahedra are found in the intermetallics KTi^8 and $CsTi^9$ both of which were found to contain isolated oblate tetragonal bipyramidal Tl_6^{6-} anions of ideal D_{4h} symmetry derived from the axial compression of a regular octahedron thereby destroying its C_3 axes. The system is modeled computationally by DFT calculations on the isolated anions Ic_6^{n-} ($Ic = B, In, Tl; z = 4, 6, 8$). The anions Ic_6^{8-} have the $14 = 2n + 2$ skeletal electron count expected for a regular octahedron and found in well-known octahedral clusters such as $B_6H_6^{2-}$. The anions Ic_6^{6-} represent the electronic configuration found in the experimentally known^{8,9} Tl_6^{6-} whereas the anions Ic_6^{4-} represent a still greater degree of electron deficiency.

2. Computational Methods

Density functional theory was used at the following two levels:

(1) B3LYP/LANL2DZ, which includes Becke's 3-parameter functional²² with LYP type nonlocal correlation functionals²³ as implemented in Gaussian 94.²⁴ The basis functions include Los Alamos ECP's and are of DZ quality.²⁵ An attempted computation on B_6^{8-} using a triple- ζ quality basis set including polarization functions did not lead to SCF convergence.

(2) A BP86 density functional with nonlocal corrections introduced in a perturbative manner coded in Spartan as pBP86/DN* using Becke's 1988 functional²⁶ with a numerical basis set (DN*) implemented in Spartan.²⁷

Since all of the electrons are not explicitly included in the B3LYP/LANL2DZ computations in contrast to the LSDA/pBP86/DN* computations, the total energies for the same species determined by the two computational methods can differ widely (see Table 1 for the In_6^{z-} species).

- Corbett, J. D. *Struct. Bonding* **1997**, 67, 175.
- King, R. B. *Inorg. Chem.* **1989**, 28, 2796.
- Muetterties, E. L.; Knoth, W. H. *Polyhedral Boranes*; Marcel Dekker: New York, 1968.
- Muetterties, E. L., Ed. *Boron Hydride Chemistry*; Academic Press: New York, 1975.
- Mingos, D. M. P.; Johnston, R. L. *Struct. Bonding* **1987**, 68, 29.
- Mingos, D. M. P.; Wales, D. J. *Introduction to Cluster Chemistry*; Prentice-Hall: Englewood Cliffs, NJ, 1990.
- Mingos, D. M. P. *Pure Appl. Chem.* **1991**, 63, 807.
- Dong, Z.; Corbett, J. D. *J. Am. Chem. Soc.* **1993**, 115, 11299.
- Dong, Z.; Corbett, J. D. *Inorg. Chem.* **1996**, 35, 2301.
- Kaskel, S.; Corbett, J. D. *Inorg. Chem.* **2000**, 39, 778.
- Huang, D.; Dong, Z.; Corbett, J. D. *Inorg. Chem.* **1998**, 37, 5881.
- Sevov, S. C.; Corbett, J. D. *J. Am. Chem. Soc.* **1993**, 115, 9089.
- Sevov, S. C.; Corbett, J. D. *Inorg. Chem.* **1993**, 32, 1059.
- Dong, Z.; Henning, R. W.; Corbett, J. D. *Inorg. Chem.* **1997**, 36, 3559.
- Sevov, S. C.; Corbett, J. D. *Inorg. Chem.* **1991**, 30, 4875.
- Sevov, S. C.; Ostenson, J. E.; Corbett, J. D. *J. Alloys Compd.* **1993**, 202, 289.
- Dong, Z.; Corbett, J. D. *J. Cluster Sci.* **1995**, 5, 187.
- Dong, Z.; Corbett, J. D. *Inorg. Chem.* **1995**, 34, 5042.
- Henning, R. W.; Corbett, J. D. *Inorg. Chem.* **1997**, 36, 6045.
- King, R. B., *Inorg. Chim. Acta* **1995**, 228, 219.
- King, R. B., *Inorg. Chim. Acta* **1996**, 252, 115.

- Becke, A. D., *J. Chem. Phys.* **1993**, 98, 5648.
- Lee, C.; Yang, W.; Parr, R. G. *Phys. Rev.* **1988**, B37, 785.
- Frisch, M. J.; Trucks, G. W.; Schlegel, H. B.; Gill, P. M. W.; Johnson, B. G.; Robb, M. A.; Cheeseman, J. R.; Keith, T.; Petersson, G. A.; Montgomery, J. A.; Raghavachari, K.; Al-Laham, M. A.; Zakrzewski, V. G.; Ortiz, J. V.; Foresman, J. B.; Peng, C. Y.; Ayala, P. Y.; Chen, W.; Wong, M. W.; Andres, J. L.; Replogle, E. S.; Gomperts, R.; Martin, R. L.; Fox, D. J.; Binkley, J. S.; Defrees, D. J.; Baker, J.; Stewart, J. J. P.; Head-Gordon, M.; Gonzalez, C.; Pople, J. A. *Gaussian 94*, Revision B.3; Gaussian, Inc.: Pittsburgh, PA, 1995.
- Hay, P. J.; Wadt, W. R. *J. Chem. Phys.* **1985**, 82, 270, 284, 299.
- Becke, A. D. *Phys. Rev.* **1988**, A38, 3098.
- Spartan version 5.1, Wavefunction, Inc., 18401 Von Karman Avenue, Suite 370, Irvine, CA 92612.

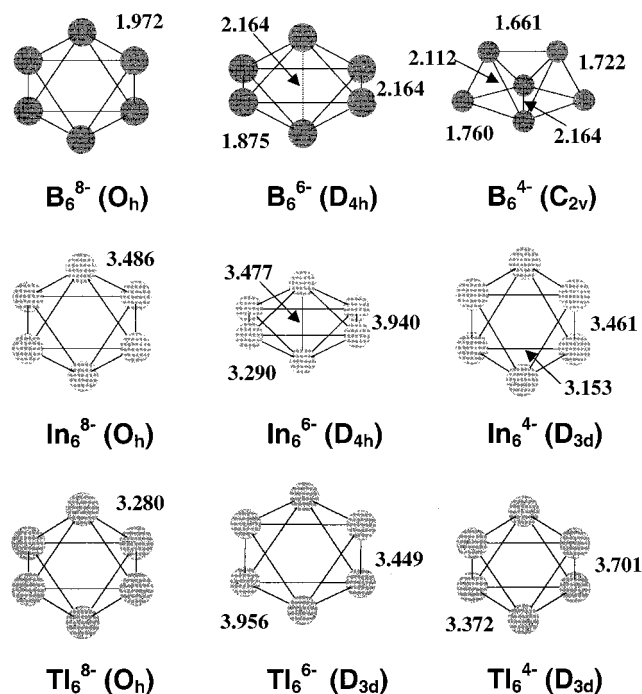


Figure 1. Optimized structures for the nine species Ic_6^{n-} ($n = 8, 6, 4$; $Ic = B, In, Tl$).

Except for Tl_6^{8-} , which converged toward the isolated atoms, all other structures have been fully optimized at both levels of approximation within the default convergence criteria found in these programs (rms gradient = 10^{-4} in Spartan; maximum force = 0.000450, rms force = 0.000300, maximum displacement = 0.001800, rms displacement = 0.001200, respectively, in Gaussian). The optimized structures are depicted in Figure 1. The computed total energies of the optimum structures of the Ic_6^{n-} species are given in Table 1.

3. Results and Discussion

3.1. The 14-Skeletal-Electron Structures Ic_6^{8-} . The optimized calculated structures for Ic_6^{8-} ($Ic = B, In$) and the experimental structure²⁸ for Tl_6^{8-} were all found to be regular octahedra in accord with their 14 skeletal electrons corresponding to the $2n + 2$ skeletal electrons required for a globally delocalized deltahedron with six vertices, namely, the regular octahedron. The computed structure for Tl_6^{8-} could not be optimized so that a single point calculation was done at the experimental geometry.²⁸

The bonding orbitals in the octahedral Ic_6^{8-} structures (see Figure 2 for the B_6^{8-} orbitals as an example) correspond to six fundamental types in increasing order of energy as follows:

(1) A low-lying a_{1g} orbital which is mainly core bonding with symmetry corresponding to the S molecular orbital of tensor surface harmonic theory (TSH).^{29–32}

(2) A degenerate triplet of t_{1u} orbitals which is heavily surface bonding but with some external bonding corresponding to P molecular orbitals of TSH.

(3) A single a_{1g} orbital which mainly contains the external lone pairs but mixed with some core bonding of opposite phase.

(4) A degenerate doublet of e_g orbitals, which contains the external lone pairs and resembles $d_{x^2-y^2}$ and d_{z^2} atomic orbitals.

(5) A degenerate triplet of t_{2g} orbitals which is exclusively surface bonding corresponding to a triplet of D molecular orbitals resembling the triplet of d_{xy} , d_{xz} , and d_{yz} atomic orbitals.

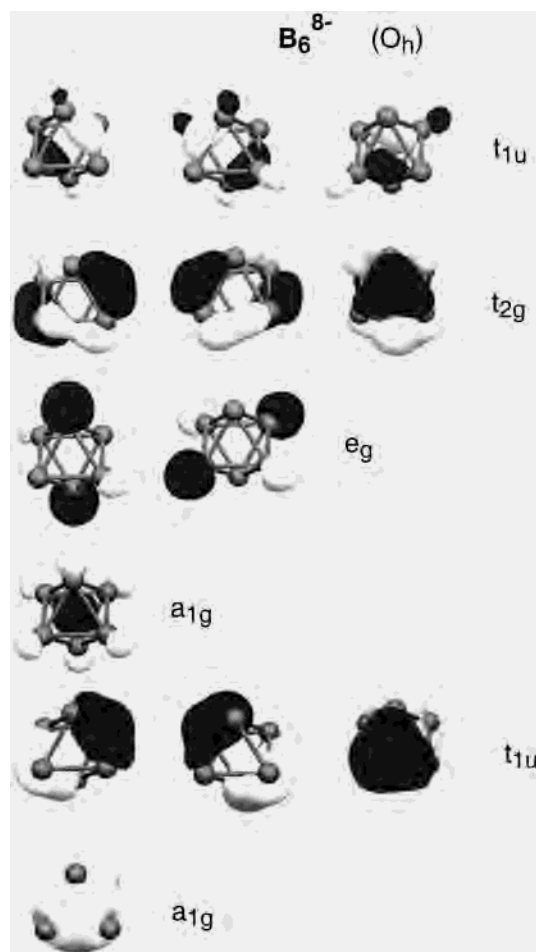


Figure 2. Bonding molecular orbitals for B_6^{8-} (O_h symmetry).

(6) A degenerate triplet of t_{1u} orbitals which is a combination of surface and external bonding resembling a degenerate triplet of f atomic orbitals.^{33–36}

Core bonding appears to be much more significant in B_6^{8-} than in its heavier congeners In_6^{8-} and Tl_6^{8-} as suggested by the following:

(1) The greater distance of the lowest lying a_{1g} orbital, corresponding almost entirely to core bonding, below the next lowest lying set of orbitals, namely, the degenerate t_{1u} triplet, corresponding only to surface and external bonding.

(2) The reversal of the relative energies of the e_g and second a_{1g} orbitals in going from B_6^{8-} to In_6^{8-} and Tl_6^{8-} . The second a_{1g} orbital obviously contains some core bonding whereas the e_g orbitals involve exclusively the external lone pairs.

3.2. The 12-Skeletal-Electron Structures Ic_6^{6-} . Removal of two skeletal electrons from Ic_6^{8-} to give Ic_6^{6-} would be expected to occur from the degenerate t_{1u} triplet HOMOs necessarily leading to a Jahn–Teller distortion corresponding to an oblate (flattened) polyhedron of some type. The optimized structures for B_6^{6-} and In_6^{6-} as well as the experimental structures for Tl_6^{6-} in KTI_8 and $CsTI_9$ were found to be oblate tetragonal bipyramids of D_{4h} symmetry. In the oblate tetragonal bipyramids for Ic_6^{6-} the axial (trans) $Ic-Ic$ distance in the

(28) Dong, Z.; Corbett, J. D. *Angew. Chem., Int. Ed. Engl.* **1996**, *35*, 1006.

(29) Stone, A. J. *Mol. Phys.* **1980**, *41*, 1339.

(30) Stone, A. J. *Inorg. Chem.* **1981**, *20*, 563.

(31) Stone, A. J.; Alderton, J. J. *Inorg. Chem.* **1982**, *21*, 2297.

(32) Stone, A. J. *Polyhedron* **1984**, *3*, 1299.

(33) Freedman, H. G., Jr.; Choppin, G. R.; Feuerbacher, D. G. *J. Chem. Educ.* **1964**, *41*, 354.

(34) Becker, C. J. *Chem. Educ.* **1964**, *41*, 358.

(35) Smith, W.; Clack, D. W. *Rev. Roum. Chim.* **1975**, *20*, 1243.

(36) King, R. B. *J. Phys. Chem. A* **1997**, *101*, 4653.

flattened direction is similar to the length of an edge (Figure 1) suggesting direct interactions between this pair of axial atoms.

Optimization of the structure of Tl_6^{6-} , like that of Tl_6^{8-} discussed above, presented some difficulties, and attempted optimization of Tl_6^{6-} starting from D_{4h} geometry failed owing to bad convergence. Introduction of artificial level shifts did not resolve this convergence problem. However, we were able to find an energy minimum for Tl_6^{6-} with D_{3d} oblate trigonal antiprismatic geometry (Figure 1) in contradiction to the experimental preference for D_{4h} oblate tetragonal antiprismatic geometry in KTl^8 and CsTl^9 . In order to clarify this discrepancy we performed a single point calculation of the energy of a D_{4h} oblate tetragonal bipyramidal Tl_6^{6-} configuration obtained from the octahedron by applying the same ratio of compression as achieved by optimized In_6^{6-} relative to In_6^{8-} . This calculation indicated that D_{4h} oblate tetragonal bipyramidal Tl_6^{6-} was approximately 6 kcal/mol higher in energy than D_{3d} oblate trigonal antiprismatic Tl_6^{6-} . This suggests that the oblate polyhedra for Ic_6^{6-} are of very similar energies so that the polyhedron of choice can be affected by the counterion and solid state environment.

The distribution of Mulliken atomic charges is particularly interesting for the two D_{4h} Ic_6^{6-} species. In the octahedral Ic_6^{8-} systems the excess negative charge is equally divided among the substituents in accord with the symmetry ($-1.333/\text{atom}$). However, in the B_6^{6-} and In_6^{6-} systems there is a distinction between the charges of the equatorial and axial atoms ($-0.895/\text{axial}$ and $-1.052/\text{equatorial}$ for B_6^{6-} and $-0.311/\text{axial}$ and $-1.345/\text{equatorial}$ for In_6^{6-}). This might be related to the short axial-axial distances calculated for B_6^{6-} and In_6^{6-} (Figure 1) since the smaller charges on the axial atoms reflect a smaller electrostatic repulsion between them, which in turn allow for the shorter trans distances between the axial atoms.

3.3. The 10-Skeletal-Electron Structures Ic_6^{4-} . In order to gain greater insight into the geometry of hypoelectronic six-vertex deltahedra, computations were also performed on the hypoelectronic 10-skeletal-electron anions Ic_6^{4-} ($\text{Ic} = \text{B}, \text{In}, \text{Tl}$), which represent a greater degree of electron deficiency than has yet been realized experimentally in isolable species. The optimized structures of the anions In_6^{4-} and Tl_6^{4-} in the B3LYP/LANL2DZ calculations were both found to be prolate (elongated) D_{3d} trigonal antiprisms, respectively. In both cases the frontier t_{1u} triplets of the corresponding regular octahedra are split into antibonding e_u doublet LUMOs and a bonding a_{2u} singlet HOMO. This corresponds to higher energy MOs

originating from the octahedral t_{1u} components along the two shorter axes of the prolate trigonal antiprisms than that of the MO originating from the third component along the longer axis.

The optimized structure for the boron analogue B_6^{4-} was found to be a C_{2v} bicapped tetrahedron (Figure 1). Conversion of an octahedron to a bicapped tetrahedron through a single diamond-square diamond process generates two degree 5 vertices. Such degree 5 vertices appear to be a particularly favorable environment for boron atoms in cluster structures as indicated by the high stability of B_{12} icosahedra in diverse structures^{37,38} and the presence of B_6 pentagonal bipyramidal building blocks in a number of optimized computed structures for large boron clusters.³⁹

The C_{2v} symmetry of the bicapped tetrahedral structure computed for B_6^{4-} means that each of its 11 bonding orbitals is nondegenerate with a unique energy. The frontier orbitals of B_6^{4-} obviously originate from the frontier t_{1u} triplet of B_6^{8-} with the b_2 component becoming the HOMO, the a_1 component becoming the LUMO, and the remaining component (b_2) being an unoccupied MO of still higher energy. A bicapped tetrahedron with equivalent edge lengths has an unsymmetrical elongated structure related to the prolate trigonal antiprisms found in the optimized structures of In_6^{4-} and Tl_6^{4-} . For this reason a bicapped tetrahedron does not appear to be unreasonable for an Ic_6^{4-} structure lacking two electron pairs for the 14-skeletal-electron closed-shell configuration of the globally delocalized octahedra of the optimized Ic_6^{8-} structures.

Acknowledgment. One of us (R.B.K.) is indebted to the Petroleum Research Fund of the American Chemical Society for partial support of this work. In addition part of this work was undertaken with the financial support from CNCSIS-Roumania, through Grant 176/4C. We are also indebted to Prof. H. F. Schaefer, III, of the University of Georgia Center for Computational Quantum Chemistry, who provided financial support for a visit of one of us (I.S.-D.) to the University of Georgia in Summer 2000. This paper was completed during this visit.

IC0009932

- (37) Jemmis, E. D.; Pavankumar, P. N. V. *Proc. Indian Acad. Sci.* **1984**, *93*, 479.
 (38) King, R. B. In *Contemporary Boron Chemistry*; Davidson, M., Hughes, A. K., Marder, T. B., Wade, K., Eds.; Royal Society of Chemistry: Cambridge, U.K., 2000; pp 506–509.
 (39) Boustani, I. *Phys. Rev. B* **1997**, *B55*, 16426.